MicroRNA-9 Targets the Neuroprotective Enzyme Glutamate Oxaloacetate Transaminase

Undergraduate Honors Research Thesis

Presented in Partial Fulfillment of the Requirements for graduation "with Honors Research Distinction" in the undergraduate School of Arts and Science of The Ohio State University.

By:
Zach Briggs

The Ohio State University

April 2016

Project Advisor: Dr. Savita Khanna, Department of Surgery

Thesis Committee:
Dr. Savita Khanna, Ph.D., Advisor
Dr. Cameron Rink, Ph.D., Co-Advisor
Dr. Gregory Booton, Ph.D.
Dr. Charles Daniels, Ph.D.

Abstract

Glutamate serves multifaceted physiological functions in the CNS as the most abundant excitatory neurotransmitter and under pathological conditions as a potent neurotoxin. Elevated extracellular glutamate is known to play a central role in ischemic brain injury. The current study stems from our key observation demonstrating that induction of glutamate oxaloacetate transaminase (GOT), a glutamate-metabolizing enzyme in the brain, can attenuate stroke-induced injury. From the historical work of Hans Krebs, we know that GOT metabolism of glutamate generates TCA cycle intermediates in brain tissue. GOT catalyzes the transfer of the amino group from glutamate to the 4-carbon TCA cycle intermediate oxaloacetate to generate aspartate and the 5-carbon TCA cycle intermediate α-ketoglutarate. We thus proposed in a previous study that induction of GOT can utilize otherwise neurotoxic glutamate to support survival of ischemic glucose-starved neural cells. The aim of the current work is to identify the mechanisms of GOT induction. Emergent literature supports microRNAs (miRNAs) as key mediators of post-transcriptional gene silencing. MicroRNAs comprise a novel class of small, noncoding endogenous RNAs that regulate gene expression by targeting mRNAs for degradation or translational repression. MicroRNA-9 (miR-9) is abundantly expressed in the brain, where it is predicted to target genes involved in glutamate metabolism. In the current work, we hypothesize that miR-9 targets GOT, resulting in post-transcriptional gene silencing. Furthermore, we hypothesize that inhibition of miR-9 upregulates GOT expression and enhances its neuroprotective properties. We recognize a therapeutic opportunity in which inhibition of miR-9 could potentially lead to improved outcome for ischemic stroke patients.

Acknowledgements

I would like to thank my advisor, Dr. Khanna, for supervising me on this project and supporting me throughout my time working in Khanna Lab. I feel that I have not only learned a lot about the complex physiology of ischemic stroke, but have also become much more proficient in performing many of the laboratory techniques that are integral to molecular biology. In addition, I have gained knowledge in the processes of experimental design, poster presentation, and writing scientific papers. I would also like to thank Dr. Rink for co-advising my project and his team in Rink Lab for supporting me in the completion of this thesis. There are far too many names to name here, but I want to thank everyone in Sen Lab who has helped train me or provide some other support over the past two years. Lastly, I want to extend my gratitude to my other two committee members—Dr. Booton and Dr. Daniels—for taking the time and effort to share the experience of defending my Honors Thesis with me.

List of Abbreviations

ATP: Adenosine triphosphate

TCA cycle: Tri-carboxylic acid cycle

ETC: Electron transport chain

NMDA: *N*-methyl-D-aspartic acid

AMPA: DL-α-amino-3-hydroxy-5-methyl-4-isoxazole propionic acid

EAAT: Excitatory amino acid transporter

ROS: Reactive oxygen species

GOT: Glutamate oxaloacetate transaminase

SO: Supplemental oxygen

RA: Room air

GFP: Green fluorescent protein

siRNA: Small-interfering RNA

miRNA: MicroRNA

RISC: RNA-induced silencing complex

3'UTR: 3'-untranslated region

MCAO: Middle cerebral artery occlusion

MRI: Magnetic resonance imaging

DICOM: Digital imaging and communications in medicine

OCT: Optimal cutting temperature

RT-PCR: Real-time polymerase chain reaction

GAPDH: Glyceraldehyde 3-phosphate dehydrogenase

Introduction

Ischemic Stroke

The impact of stroke on American society is staggering. Each year, more than 795,000 people are afflicted by and more than 130,000 people are killed by stroke[1,2]. This makes stroke the fifth leading cause of death in the United States[1]. In addition, the annual cost of healthcare services, medications, and missed days of work associated with stroke is approximately $34 billion[3]. Given the severity of the burden of stroke on people's personal lives, the healthcare system, and the U.S. economy, it should not be surprising that the number of publications from stroke-related studies has doubled from 2005 to 2015[4].

There are two types of stroke: ischemic and hemorrhagic **(Figure 1)**. Hemorrhagic strokes are caused by rupturing of blood vessels in the brain, while ischemic stroke is characterized by a lack of blood flow to the brain. The latter may be caused by factors such as a blood clot that forms in the brain. In either case, the result is a shortage of oxygen and glucose delivery to neural cells. This is especially problematic considering that the brain uses 20-25% of the body's total oxygen intake and that glucose is the primary metabolic fuel for neurons[5]. Of interest for this study are ischemic strokes, which constitute 87% of stroke cases[3].

Glucose and oxygen are both essential to the metabolic pathway that ultimately produces adenosine triphosphate (ATP). During glycolysis, glucose is oxidized to pyruvate. Pyruvate is then converted into acetyl-CoA, which enters the tri-carboxylic acid (TCA) cycle. This eight-reaction cycle produces the electron donors NADH and $FADH_2$, which feed into the electron transport chain (ETC). Molecular oxygen (O_2) is the final electron acceptor in the ETC, and the

proton gradient that is established across the inner mitochondrial membrane leads to the production of ATP by the enzyme ATP synthase. Overall, two molecules of ATP are produced during glycolysis, two are produced during the TCA cycle, and 28 are produced during oxidative phosphorylation by ATP synthase.

ATP is necessary for the functioning of the sodium/potassium ATPase (Na^+/K^+ ATPase). This ion pump maintains proper ionic balance across the neuronal cell membrane by transporting three Na^+ ions out of the cell and two K^+ ions into the cell through the consumption of one ATP molecule. Under the hypoxic and hypoglycemic conditions of ischemia, ATP production is significantly reduced. This prevents the Na^+/K^+ ATPase from properly functioning, causing sodium and potassium to move passively down their electrochemical gradients. The cell membrane potential is normally approximately -70 mV, so the electrochemical gradient for Na^+ into the cell is greater than the electrochemical gradient for K^+ out of the cell. Na^+ thus moves intracellularly faster than K^+ moves extracellularly. The resulting ionic imbalance depolarizes the cell membrane. The change in membrane potential opens voltage-gated calcium (Ca^{2+}) channels at the axon terminals of the presynaptic neuron. There is a large influx of Ca^{2+} into the presynaptic neuron, leading to the release of neurotransmitters into the synapse via synaptic vesicles. The neurotransmitter of interest for the current study is the amino acid glutamate, which is described below.

Glutamate

In addition to being one of the twenty amino acids found in eukaryotic proteins, glutamate also functions as an excitatory neurotransmitter in the mammalian central nervous system[5]. Under

normal physiological conditions, glutamate plays an important role in cognitive processes such as learning and memory[6]. When glutamate is released into the synapse from vesicles in the presynaptic neuron, it binds to ionotropic receptors on the postsynaptic cell membrane **(Figure 2)**. These include *N*-methyl-D-aspartic acid (NMDA) and DL-α-amino-3-hydroxy-5-methyl-4-isoxazole propionic acid (AMPA)[5]. The binding of glutamate to NMDA and AMPA initiates an action potential in the postsynaptic neuron and further propagates signal transduction. In order to prevent overstimulation of the glutamatergic receptors, glutamate is cleared from the synapse by a group of transmembrane proteins called excitatory amino acid transporters (EAATs)[5]. While different members of this protein family are found on both neurons and glial cells, EAAT2—which is present in astrocytes—is the primary transporter of glutamate from the synapse[7,8].

Under the pathological conditions of ischemic stroke, glutamate becomes neurotoxic due to its accumulation in the synapse **(Figure 3)**. In the absence of ATP production, depolarization of the presynaptic neuron leads to an influx of calcium, causing an excessive release of glutamate from presynaptic vesicles. In addition, the EAATs are active transporters, moving glutamate intracellularly against its concentration gradient. These transporters fail to function properly under ischemic conditions due to the lack of ATP production. Glutamate thus moves down its concentration gradient from the astrocytes to the extracellular space, further exacerbating glutamate accumulation at the synapse[5].

The excessive glutamate levels overwhelm the chemically-gated AMPA receptors. AMPA is an ion channel that opens upon binding to glutamate, leading to the influx of positive ions into the postsynaptic neuron. The resulting increase in cell voltage opens the voltage-gated NMDA

receptors, which also function as ion channels. Excessive levels of calcium flow intracellularly through these receptors and activate proteases, endonucleases, phospholipases, and nitric oxide synthase, the latter leading to the production of reactive oxygen species (ROS) such as nitric oxide, superoxide, and hydrogen peroxide. The activation of these enzymes and ROS causes oxidative stress by reacting with the cell's DNA, plasma membrane, cytoskeleton, and other structures vital to the cell's survival. The cell ultimately dies as a result[5]. Glutamate thus plays an important role in the pathophysiological cascade that leads to the necrosis that is characteristic of ischemic stroke **(Figure 4)**.

Given glutamate's neurotoxic role in ischemic stroke, it is not surprising that a variety of studies have been performed with the goal of reducing glutamate accumulation at the synapse during ischemia. These studies have largely focused on targeting the transmembrane proteins that directly interact with glutamate at the synapse[5]. Drugs have been designed with the intention of blocking glutamate receptors, blocking ion channels, or upregulating the expression of EAATs. While these research efforts have had success in preclinical trials, they have failed to translate into clinical success[9,10,11]. What these studies have in common is that they are attempting to address the downstream events of the ischemic cascade without addressing the original problem: lack of glucose delivery to the brain. Without glucose, the processes of glycolysis, the TCA cycle, and oxidative phosphorylation which produce ATP cannot take place. However, cells are capable of metabolizing other compounds under hypoglycemic conditions, including amino acids such as glutamate. Glutamate can be metabolized into the TCA cycle by an enzyme called glutamate oxaloacetate transaminase (GOT). This enzyme and its implications in the current study are described below.

Glutamate Oxaloacetate Transaminase (GOT)

The current work is based on a transcriptome screening of mouse and rat brain during ischemic stroke previously performed by our lab. That study demonstrated that levels of the enzyme glutamate oxaloacetate transaminase (GOT) were significantly increased in the stroke-affected hemisphere in animals receiving supplemental oxygen (SO) (inhaling 100% O_2) during ischemia compared to those exposed to normal room air (RA) conditions[12]. Thus, correction of hypoxia during ischemic stroke induces GOT expression.

GOT catalyzes the transfer of the amino group from glutamate to the 4-carbon TCA cycle intermediate oxaloacetate to form the amino acid aspartate and the 5-carbon TCA cycle intermediate α-ketoglutarate **(Figure 5)**. Thus, glutamate can serve as a substrate to allow a truncated version of the TCA cycle to proceed **(Figure 6)**. The reaction between acetyl-CoA and oxaloacetate to form citrate, and the subsequent formations of cis-aconitate and isocitrate, are bypassed.

Delivery of glucose to brain tissue is drastically reduced under ischemic conditions due to the lack of blood supply. Thus, neurons and glial cells are unable to utilize their primary metabolic fuel. During ischemic stroke, glutamate accumulates in the synapses at neurotoxic levels and contributes to the pathophysiological cascade that ultimately results in cell death. GOT is capable of metabolizing glutamate into a truncated version of the TCA cycle, a process that normally depends on the presence of glucose. Taking all of this together, our lab built off of the transcriptome screening study to propose that, under the hypoglycemic conditions of ischemic

stroke, correction of hypoxia can induce GOT expression, allowing the enzyme to metabolize glutamate and protect the brain from stroke-induced injury[13].

In this study, rats were exposed to either RA conditions or SO during experimentally induced ischemic stroke. GOT mRNA expression, enzyme activity, and protein expression were significantly increased in the stroke-affected hemisphere of rats exposed to SO compared to the contralateral hemisphere and the stroke-affected hemisphere of RA controls **(Figure 7)**. In addition, glutamate levels in the stroke-affected hemisphere of SO rats were significantly lower than that of RA controls. Rats exposed to RA conditions also experienced a reduction in ATP levels in the stroke-affected hemisphere compared to the contralateral, while ATP levels were approximately equal in both hemispheres for rats exposed to SO **(Figure 8)**. These results support the idea that GOT metabolizes glutamate upon correction of hypoxia during ischemic stroke.

The implications of GOT in ischemic stroke are relevant in mice as well, the model for the current work. The study described in the previous paragraph used a second *in vivo* model in which mice were subjected to ischemic stroke under SO conditions. One week before ischemia was induced, mice were given green fluorescent protein (GFP)-tagged lentiviral vectors containing either GOT overexpression, knockdown, or scramble (control) small-interfering RNA (siRNA). The control siRNA had no effect on GOT mRNA expression or lesion volume of the stroke-affected hemisphere. GOT overexpression significantly increased GOT mRNA expression and reduced the lesion volume of the stroke-affected hemisphere. In contrast, GOT knockdown resulted in death from ischemia-induced brain injury for five of the six mice receiving this

vector. For the lone survivor, GOT mRNA expression was significantly reduced in the stroke-affected hemisphere and the lesion volume was drastically increased **(Figure 9)**.

Our lab is now investigating other mechanisms of GOT induction. The current study proposes that GOT is a target of miR-9—a member of a larger class of RNAs known as microRNAs (miRNAs).

microRNAs and miR-9

MicroRNAs (miRNAs) are endogenous, noncoding RNA molecules approximately 22 nucleotides in length. They play an important role in gene regulation in plants and animals. Specific functions of miRNAs have been elucidated in a variety of organisms, ranging in complexity from *C. elegans* to humans[14].

miRNA genes are transcribed primarily by RNA polymerase II, forming a precursor molecule called a pri-miRNA. After the pri-miRNA is transcribed, it is cleaved by the Drosha RNase III endonuclease[14]. The cut creates a stem loop secondary structure about 60-70 nucleotides in length. This miRNA precursor—known as a pre-miRNA—is transported from the nucleus to the cytosol using the nuclear export receptor Exportin-5[15,16]. Once in the cytoplasm, the double-stranded portion of the stem loop is recognized by the enzyme Dicer[14]. Dicer then cuts both strands, eliminating the loop and creating an imperfect duplex. Only one of the two strands will become the mature gene product: this strand is the miRNA, while the other strand is called the miRNA*[17]. The strands of the miRNA:miRNA* duplex are then separated[14]. The miRNA strand is loaded into the RNA-induced silencing complex (RISC), while the miRNA* strand is

degraded. After the mature miRNA is loaded into the RISC, the enzyme complex is ready to act on a target mRNA. The miRNA targets an mRNA message for either degradation or translational repression by binding to the 3'-untranslated region (3'UTR) of the mRNA[18]. The pathway of miRNA processing—from transcription to mRNA targeting—is shown in **Figure 10**.

The present study focuses on microRNA-9 (miR-9), which is specifically expressed in the central nervous system of vertebrates[19]. It has been found to play an important role in a number of neurodegenerative disorders, including Huntington's disease[20,21,22], Alzheimer's disease[23,24], amyotrophic lateral sclerosis (ALS)[25], and Parkinson's disease[26]. In mice and humans, the miR-9 gene has three predicted stem loop precursor structures, which are denoted miR-9-1, miR-9-2, and miR-9-3. These three predicted stem loops—along with the mature miR-9 and miR-9* sequences—are depicted in **Figure 11**.

As shown in **Table 1**, different miRNAs have been implicated in ischemic stroke in terms of risk factors for onset of stroke and components of the ischemic pathophysiological cascade[27]. In December 2015, a paper published by Wei et al. was made available on Pubmed ahead of print. It is the first publication to report a link between miR-9 and stroke[28]. This study showed that miR-9 is downregulated under the hypoxic and hypoglycemic conditions of ischemia, and that it mediates neuronal apoptosis under these conditions by targeting a gene called Bcl2l11. The current study also focuses on the implications of miR-9 in stroke, but from the more upstream perspective of restoring metabolic fuel for brain tissue in the absence of glucose. Here, we propose that the mRNA of GOT—the enzyme that we have previously shown to promote cell

survival during ischemia by metabolizing neurotoxic glutamate into the TCA cycle—is a target of miR-9.

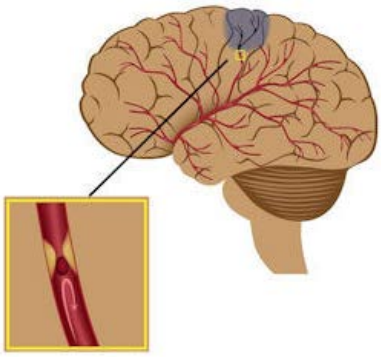

Ischemic Stroke

- Blockage of blood vessel in brain
- 87% Occurrence
- 7.6% Mortality Rate

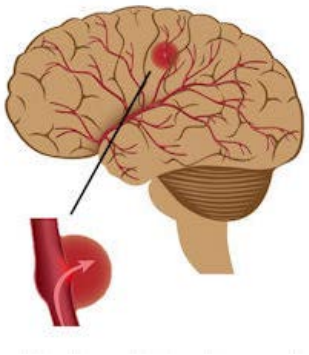

Hemorrhagic Stroke

- Rupturing of blood vessel in brain
- 13% Occurrence
- 37.5% Mortality Rate

Figure 1: Differences between Ischemic and Hemorrhagic Stroke

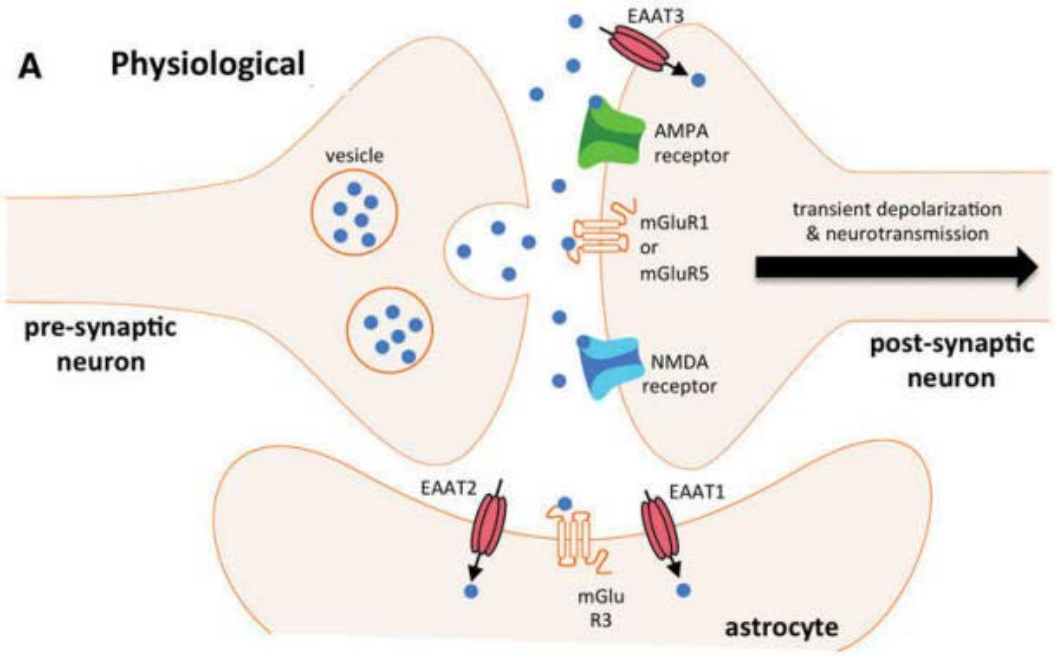

Figure 2: Tripartite synapse under physiological conditions. Under physiological conditions, glutamate serves as the most abundant excitatory neurotransmitter in the brain. Sequestered in vesicles of the pre-synaptic neuron, glutamate is released into the synaptic cleft upon depolarization. Once released, glutamate binds to ionotropic (*i.e.*, NMDA, AMPA) and/or metabotropic receptors (*i.e.*, mGluR1, mGluR5) of the post-synaptic neuron to potentiate signal transduction. Glutamate clearance from the synaptic cleft is primarily handled by astrocyte-specific excitatory amino acid transporters (*i.e.*, EAAT2). Adapted from Ref 5.

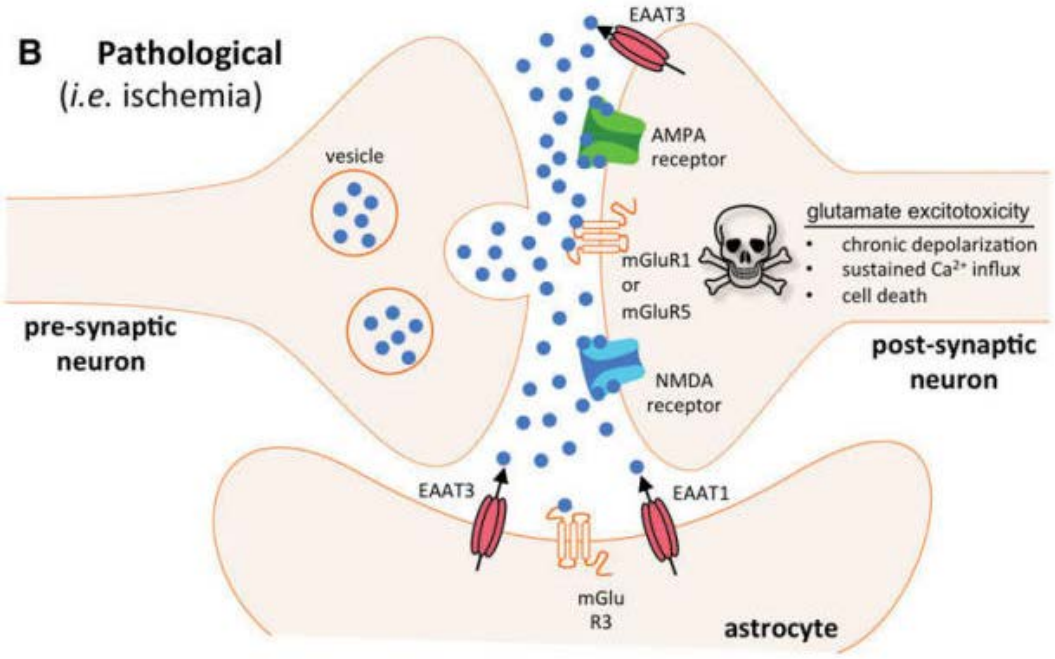

Figure 3: Tripartite synapse under pathological conditions of acute ischemic stroke. Under pathological conditions of cerebral ischemia, energetic failure leads to reversal of EAATs and accumulation of glutamate in the synaptic cleft. Excitotoxic stimulation of glutamate receptors results in chronic depolarization, sustained Ca^{2+} influx, and cell death. AMPA, DL-α-amino-3-hydroxy-5-methyl-4-isoxazole propionic acid; EAAT, excitatory amino acid transporter; NMDA, *N*-methyl-D-aspartic acid. Adapted from Ref 5.

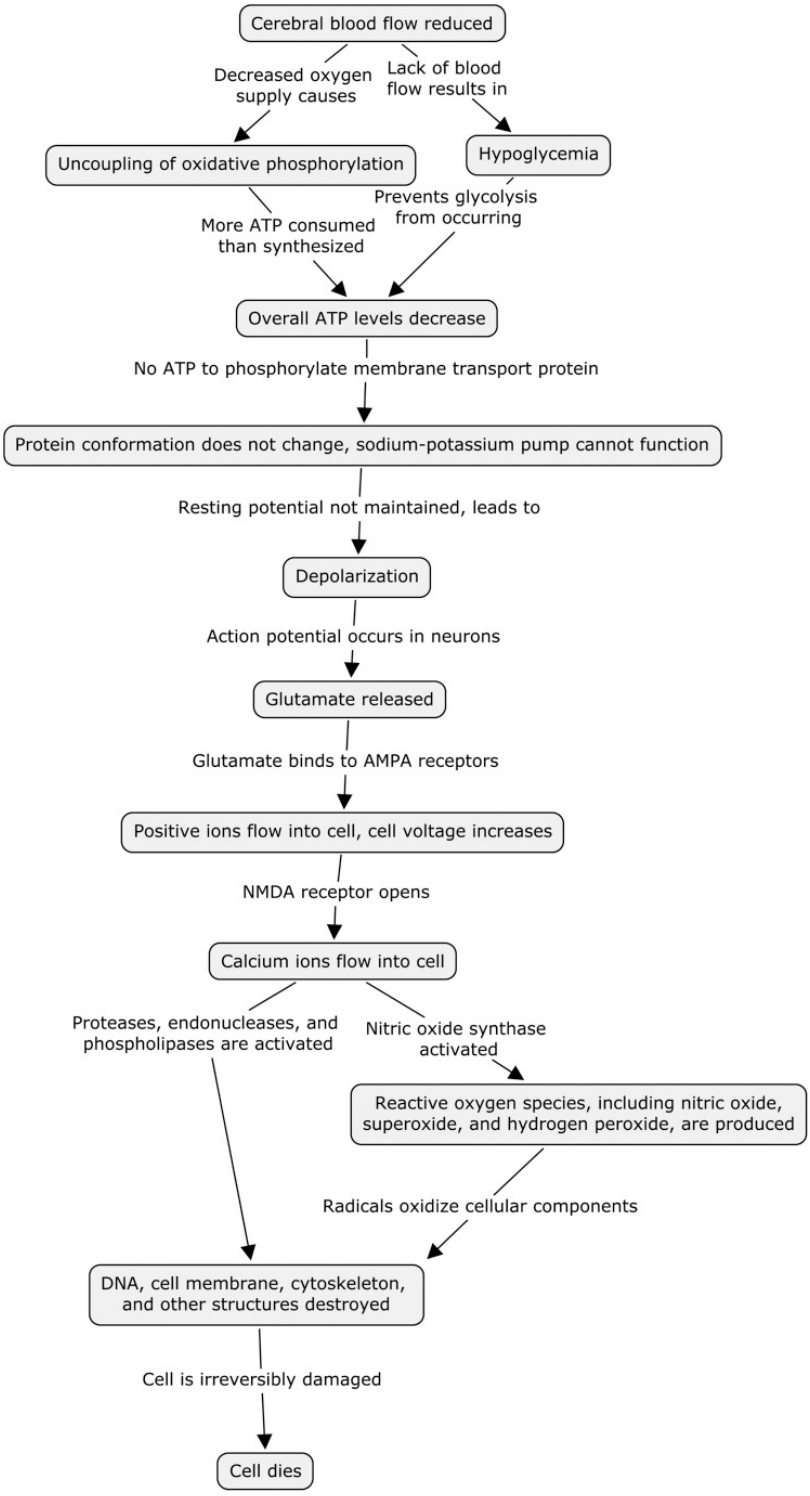

Figure 4: Ischemic cascade in neural cells. Cerebral ischemia results in a pathological cascade of cellular events triggered by energetic failure that lead to glutamate excitotoxicity and culminate in cell death. Adapted from Ref 5.

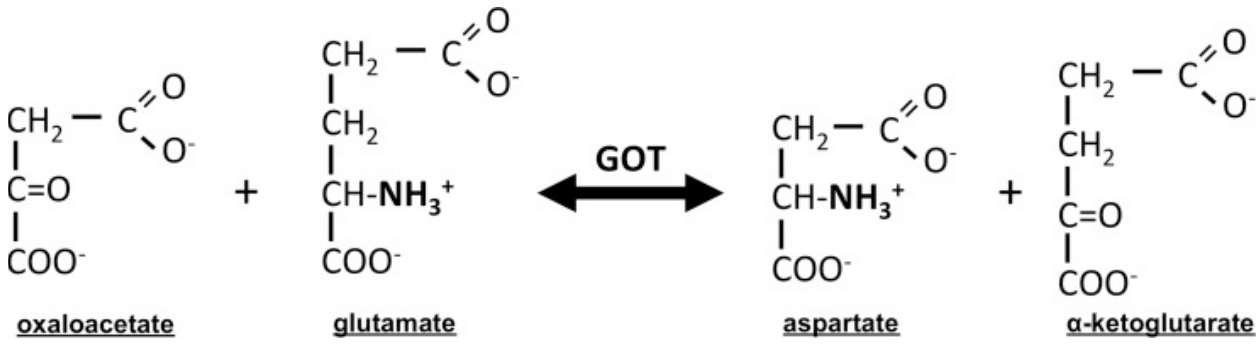

Figure 5: Glutamate oxaloacetate transaminase. GOT catalyzes the reversible transfer of an amino group (NH_3^+) from glutamate to the four-carbon TCA cycle intermediate oxaloacetate to generate aspartate and the five-carbon TCA cycle intermediate α-ketoglutarate. GOT, glutamate oxaloacetate transaminase; TCA, tri-carboxylic acid. Adapted from Ref. 5.

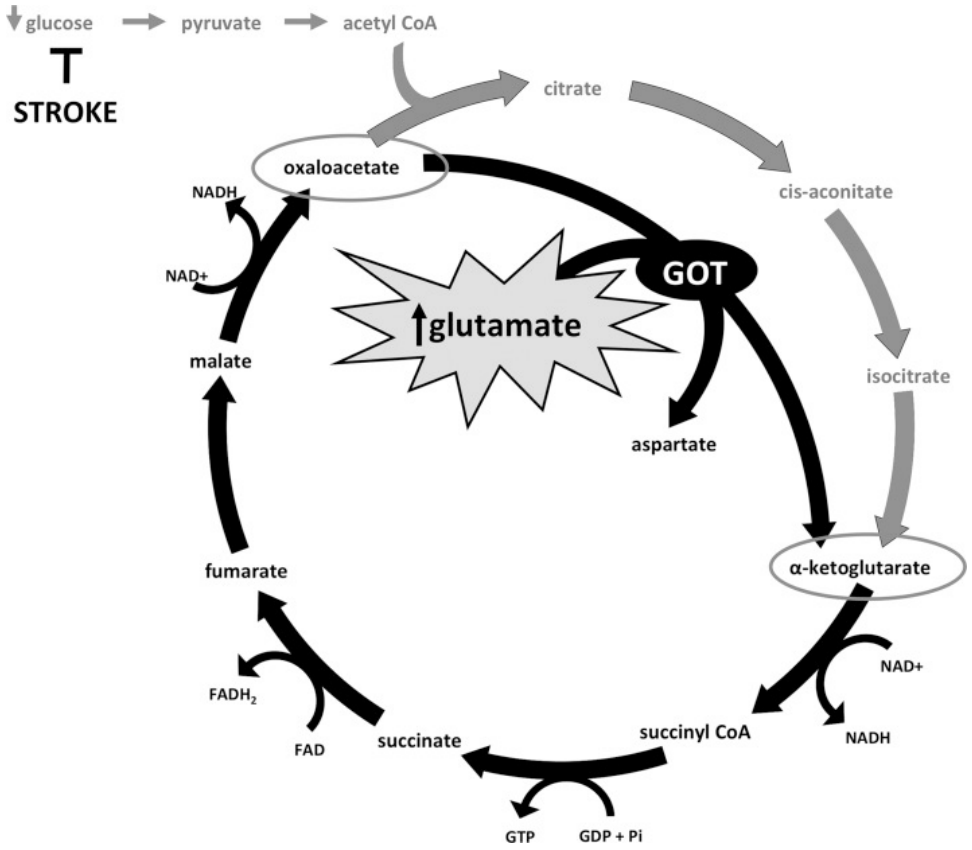

Figure 6: GOT enables an abridged TCA cycle. In the absence of glucose during ischemic stroke, neural cells that lack glycogen stores must turn to alternative substrates to maintain cellular energetics. We hypothesize that GOT enables an abridged TCA cycle under conditions of stroke-induced hypoglycemia such that otherwise excitotoxic glutamate undergoes a role reversal to become a source of energy and survival factor. Adapted from Ref 5.

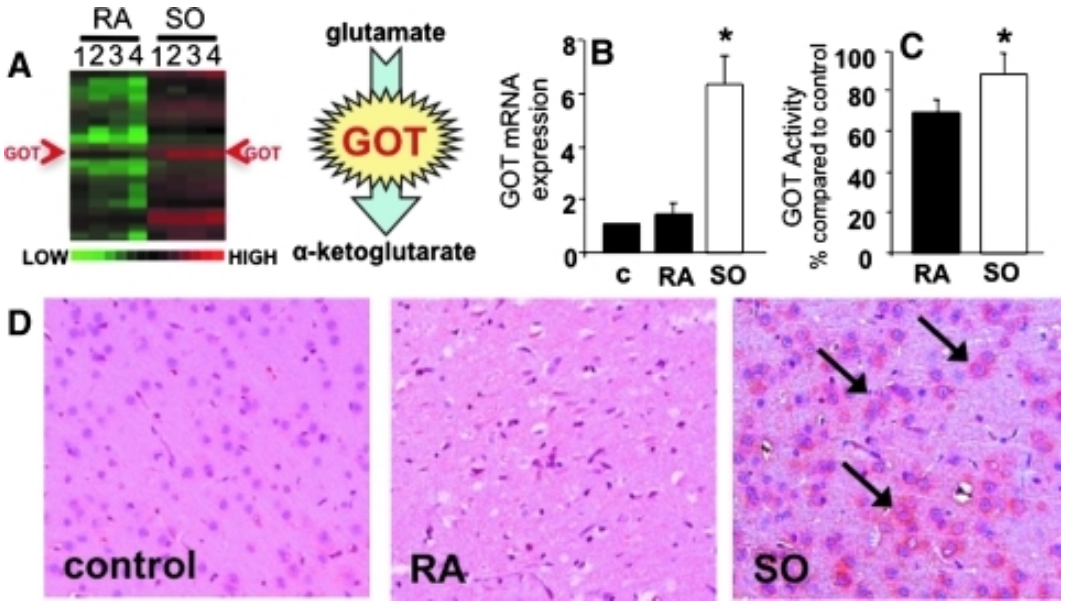

Figure 7: Correction of stroke-induced hypoxia increases GOT expression and activity at stroke site. The rodent brain transcriptome was compared between normoxic (RA) and SO groups. **(A)** Heat map—from 3281 genes with higher expression in SO-treated stroke tissue as compared to RA, GOT was identified as a gene target for the ability to metabolize Glu into tricarboxylic acid cycle intermediates. **(B)** GOT gene expression was validated in contralateral control (c), RA and SO neurons laser captured from cortex. **(C)** GOT activity and **(D)** immunostaining were significantly higher in SO than in RA stroke tissue. *p<0.05. c, control; Glu, glutamate; GOT, glutamate oxaloacetate transaminase; RA, room air; SO, supplemental oxygen. Adapted from Ref 13.

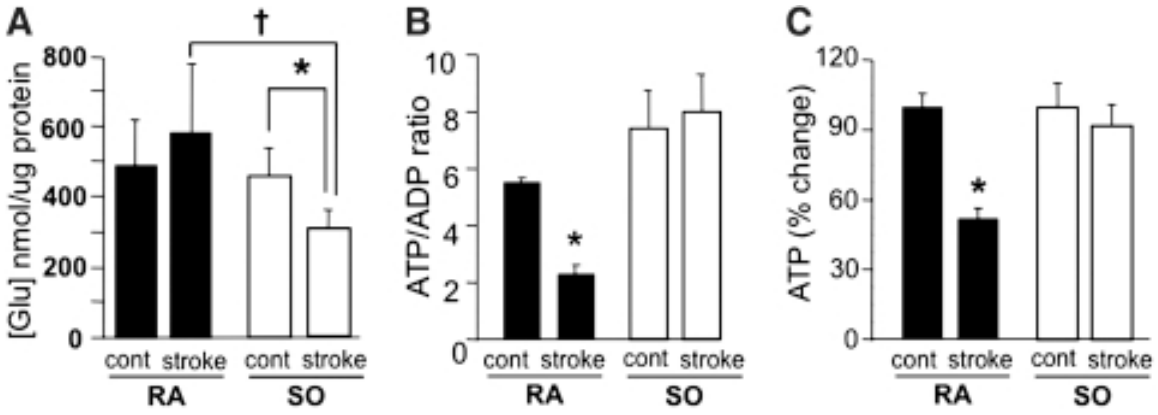

Figure 8: SO lowered cortical Glu concentration and protected against loss of ATP in stroke affected brain tissue. S1 cortex in contralateral and stroke-affected tissue after 90 min MCAO without reperfusion under RA or SO. Assays: **(A)** Glu concentration, **(B)** ATP/ADP, and **(C)** ATP% change. $p<0.05$: *control versus stroke, †RA stroke versus SO stroke. MCAO, middle cerebral artery occlusion. Adapted from Ref 13.

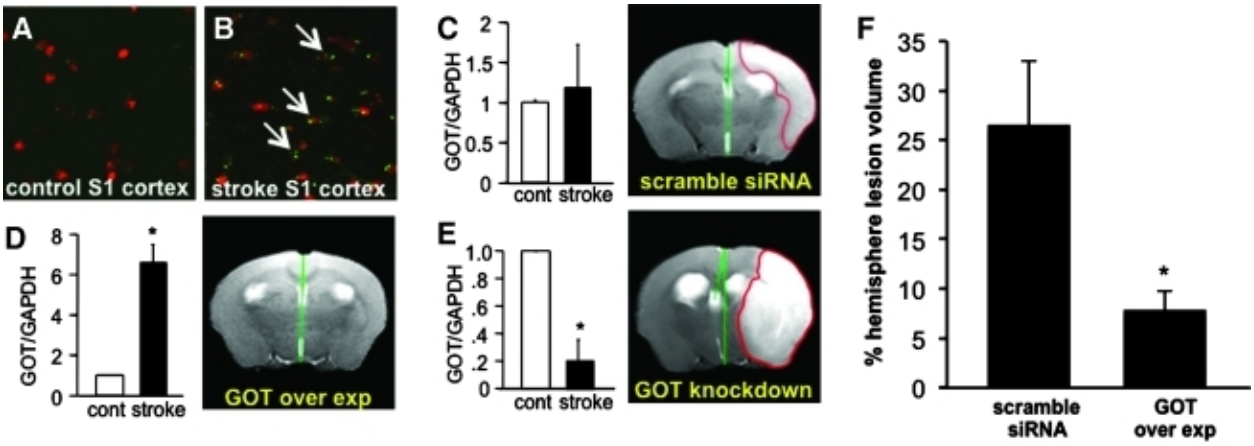

G

lentiviral vector	n	successful MCAO	48h survival & MRI
scramble siRNA control	3	3/3 (100%)	3/3 (100%)
GOT over-expressing	6	6/6 (100%)	5/6 (83%)
GOT knockdown	6	6/6 (100%)	1/6 (17%)

Figure 9: GOT overexpression and knockdown influenced stroke outcome under SO conditions. GFP-tagged lentiviral vector delivered to cortex transduced 25–35 mm^3 of brain tissue covering the stroke area. **(A, B)** GFP and NeuN (red) coexpression in S1 cortex of stroke hemisphere (arrow) was >95% compared to control. One week after lentiviral injection, mice were subjected to MCAO with correction of hypoxia by SO during cerebral ischemia. **(C–E)** GOT mRNA expression from right (stroke) and left (contralateral control) hemisphere and representative 11.7T 48 h MRI of **(C)** control (iLenti-GFP scrambled siRNA), **(D)** GOT overexpression, and **(E)** GOT knockdown mice. **(F)** Digital planimetry of T2-weighted 48 h MRI was employed to determine stroke-induced lesion volume as percentage of hemisphere. **(G)** Successful MCAO was confirmed by laser Doppler flowmetry. Only one of six GOT knockdown mice survived to 48 h MRI. **p*<0.05 control versus stroke. MRI, magnetic resonance imaging. Adapted from Ref 13.

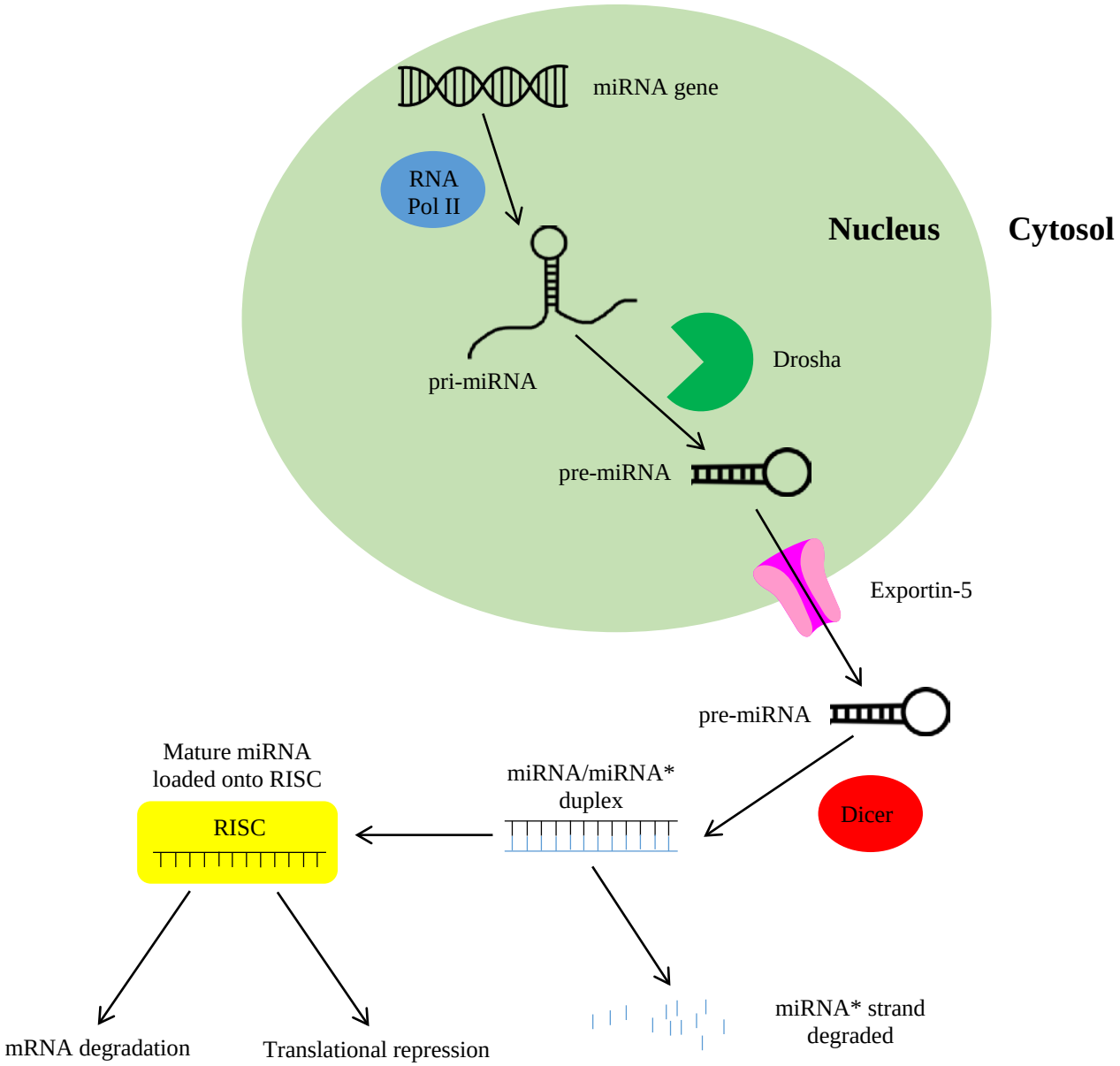

Figure 10: miRNA Transcription, Maturation, and mRNA Targeting.

mmu-miR-9-1

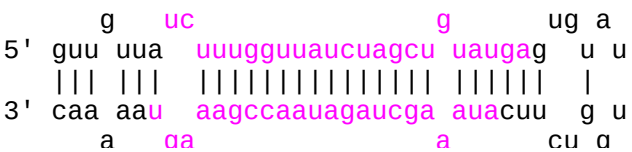

mmu-miR-9-2

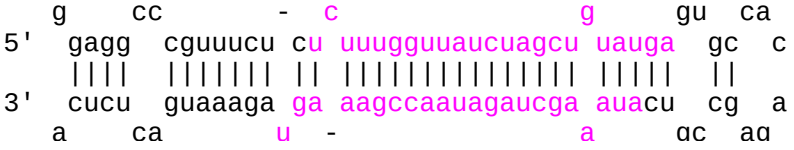

mmu-miR-9-3

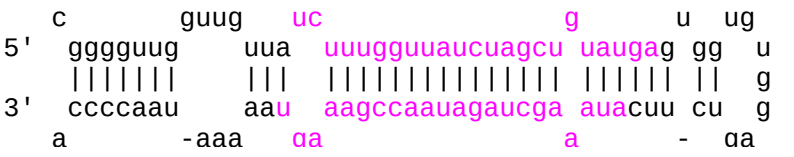

Figure 11: Secondary Stem Loop Structures of the Three Mouse miR-9 Gene Products. The bases highlighted in pink indicate the sequences of the 5' arm and the 3' arm of the mature miRNA, which are the same for all three miR-9 genes. Obtained from miRBase.

miRNA	Stroke Risk Factor/Event in Pathophysiological Cascade
miR-21[29,30]	Atherosclerosis[29,30]
miR-126[31,32]	Atherosclerosis[31,32]
miR-33[33]	Hyperlipidemia[33]
miR-125a-5p[34]	Hyperlipidemia[34]
miR-155[35,36]	Hypertension[35,36]
miR-222[37,38]	Plaque rupture[37,38]
miR-210[39,40]	Plaque rupture[39,40]
miR-15a[41]	Blood brain barrier disruption[41]
miR-497[42]	Cell apoptosis[42]
miR-9[28]	Cell apoptosis[28]

Table 1: Implication of miRNAs in Ischemic Stroke.

Materials and Methods

Cell Culture

Mouse hippocampal HT4 neural cells were grown in Dulbecco's modified Eagle medium supplemented with 10% fetal calf serum, 100 μg/mL streptomycin, 100 units/mL penicillin, and 0.25 μg/mL amphotericin at 37ºC in a humidified atmosphere of 95% air and 5% CO_2. Immediately before starting the experiments, the culture medium was replaced with fresh medium containing the same supplement conditions[43].

Transfection

HT4 neural cells (0.1×10^6 cells/well in 12-well plate) were seeded in antibiotic-free medium for 24 hours before transfection. DharmaFECT 1 transfection reagent was used to transfect cells with miRIDIAN mmu-miR-9 mimic or miRIDIAN mmu-miR-9 inhibitor (Thermo Scientific Dharmacon RNA Technologies, Lafayette, CO, USA) according to the manufacturer's instructions. miRIDIAN miR mimic or inhibitor negative control (Thermo Scientific Dharmacon RNA Technologies, Lafayette, CO, USA) were used for control transfections. After 72 hours, RNA or protein were isolated from the cells[43].

Dual Luciferase Assay

After 72 hours of transfection with mmu-miR-9 mimic or mmu-miR-9 inhibitor, HT4 cells were transfected with 100 ng of pLuc-GOT—3'UTR plasmid (Signosis, Santa Clara, CA). Normalization was achieved by co-transfection with *Renilla* plasmid (10 ng). Cells were lysed after 24 hours, and luciferase activity was determined using the dual-luciferase reporter assay

system (Promega, Madison, WI). Data are presented as ratio of Firefly:*Renilla* luciferase activity[44].

RNA Isolation and Real-Time PCR

Total RNA was extracted using the miRVana miRNA Isolation Kit according to the manufacturer's protocol (Ambion, Grand Island, NY, USA). Specific TaqMan assays for miRs and the TaqMan Micro-RNA Reverse Transcription Kit were used to determine miR expression, followed by real-time PCR using the Universal PCR Master Mix (Applied Biosystems, Grand Island, NY, USA). Levels of miRNA were quantified with the relative quantification method using miR-16 as the housekeeping miRNA. Relative quantification method 2 ($\Delta\Delta$ct) was employed for miRNA expression levels[43].

Western Blot

After protein extraction, protein concentrations were determined using the BCA protein assay (Pierce Chemical Co., Rockford, IL). Samples (20-30 μg of protein/lane) were separated on a 10% SDS-polyacrylamide gel electrophoresis, and probed with anti-GOT (1:1000, Abcam, Cambridge, MA). Membranes were probed with anti-GAPDH antibody to normalize (1:10000, Sigma-Aldrich, St. Louis, MO)[43].

Stereotaxic Delivery of Lentiviral Particles

To knockdown miR-9, a 10-μL syringe connected to a motorized nano-injector (KD Scientific, Holliston, MA, USA) was used to deliver 5 μL of GFP-tagged miR-9 inhibitor lentiviral transduction particles or non-targeting scramble control lentiviral particles (1.0×10^8 IU/mL,

Applied Biological Materials, Richmond, British Columbia) at a rate of 0.2 μL/minute by stereotaxic injection. Lentiviral particles were delivered to the somatosensory cortex (S1) of the anticipated stroke hemisphere using the following coordinates: –0.5mm posterior, +3.5mm lateral, and –1.0mm ventral to bregma. MCAO was performed on mice after 72 hours of delivery[13].

Mouse Stroke Model

Focal cerebral ischemia was induced in 8- to 10-week-old C57BL/6 mice by the intraluminal suture method of middle cerebral artery occlusion (MCAO) for 60 minutes. Laser Doppler flowmetry (DRT4, Moor Instruments, Wilmington, DE, USA) was used to confirm successful MCAO (70±10% drop in MCA territory cerebral blood flow)[43].

Magnetic Resonance Imaging and Determination of Infarct Volume

T2-weighted magnetic resonance imaging (MRI) was performed on mice 48 hours post-stroke using an 11.7 (500 MHz) MR system comprised of a vertical bore magnet (Bruker Biospin, Ettlingen, Germany) to determine infarct volume. To perform stroke-volume calculations, raw MRI images were converted to digital imaging and communications in medicine (DICOM) format and read into ImageJ software (NIH). After matched contrast enhancement of images in ImageJ, digital planimetry was performed by a masked observer to delineate the infarct area in each coronal brain slice. Infarct areas from brain slices were summed, multiplied by slice thickness, and corrected for edema-induced swelling to determine infarct volume[13].

Tissue Processing and Sectioning, Immunofluorescence, and Microscopy

Immediately following MRI, mouse brain tissue was harvested, sliced using a brain matrix (Ted Pella, Redding, CA, USA) and embedded in optimal cutting temperature (OCT) compound. OCT-embedded frozen brain was sectioned at 12 μm and mounted onto slides. Coronal brain sections were stained with anti-GOT antibody (1:200, Abcam, Cambridge, MA). Stained sections were analyzed by fluorescence microscopy (Axiovert 200 M, Zeiss, Gottingen, Germany) and images were captured using Axiovert v4.8 software (Zeiss)[43].

Statistical Analysis

Data are reported as mean±S.D. of at least three experiments. Difference in means was tested using Student's t-test or one-way ANOVA followed by Scheffe's *post hoc* test. $p<0.05$ was considered statistically significant[43].

Results

The current work hypothesizes that miR-9 targets the glutamate-metabolizing, neuroprotective enzyme GOT. MicroRNAs bind to the 3'UTRs of the mRNAs of the genes that they regulate. This targets the mRNAs for either degradation or translational repression. We thus wanted to demonstrate that targeting of GOT mRNA by miR-9 was possible by computationally screening for sites of complementarity between miR-9 and the 3'UTR of GOT. Two different algorithms—Targetscan Mouse (version 5.1) and miRanda—were used to search for such regions of complementarity. Both algorithms showed perfect complementarity between bases 24-30 of the 3'UTR of GOT and bases 2-8 of miR-9 **(Figure 12)**. Residues 2-8 of miRNAs are known to be particularly important in binding to mRNA targets[29]. This region of a miRNA is known as the seed sequence. Given that only the seed sequence of miR-9 shows complementarity with the 3'UTR of GOT, the GOT mRNA would be referred to as a 5'-dominant seed-only target site[29]. This *in silico* approach therefore demonstrates that miR-9 and GOT have sufficient binding complementarity for targeting of the latter by the former to be possible.

To test the hypothesis that miR-9 targets GOT, we employed an *in vitro* model and an *in vivo* model. For the former, mouse hippocampal HT4 cells were used. Experimental cells were transfected with either miRIDIAN mmu-miR-9 mimic to simulate upregulation of miR-9 expression or miRIDIAN mmu-miR-9 inhibitor to simulate downregulation of miR-9 expression. Control cells were transfected with either control mimic or control inhibitor.

After 72 hours of transfection, RNA or protein were isolated from HT4 cells. miR-9 expression levels were determined by real-time polymerase chain reaction (RT-PCR). As expected, miR-9

expression was significantly increased in cells transfected with mmu-miR-9 mimic compared to controls **(Figure 13A)**. Likewise, miR-9 expression was significantly reduced in cells transfected with mmu-miR-9 inhibitor compared to controls **(Figure 13B)**. GOT expression levels in transfected cells were measured using Western blot. Glyceraldehyde 3-phosphate dehydrogenase (GAPDH) was used as a housekeeping protein to normalize the data. GOT expression in cells transfected with mmu-miR-9 mimic was less compared to that in the control mimic cells **(Figure 13C)**. Conversely, GOT expression in cells transfected with mmu-miR-9 inhibitor was greater compared to that in control inhibitor cells **(Figure 13D)**. This suggests that miR-9 and GOT expression levels are inversely related.

To demonstrate that miR-9 targets GOT, mmu-miR-9 mimic cells and control mimic cells were co-transfected with pLuc-GOT—3'UTR plasmid and *Renilla* plasmid for 24 hours. The GOT plasmid contained Firefly luciferase as part of the construct, while the *Renilla* plasmid contained *Renilla* luciferase. After 24 hours, the cells were lysed and a dual luciferase assay was performed. The data were collected as the ratio of Firefly:*Renilla* luciferase enzyme activity. A greater ratio would correspond to a greater amount of GOT expression. The Firefly:*Renilla* luciferase ratio was found to be significantly lower in mmu-miR-9 mimic cells compared to mimic controls **(Figure 14)**. The dual luciferase assay suggests that miR-9 targets GOT *in vitro*.

GOT protects the brain from injury during ischemic stroke by metabolizing glutamate into the TCA cycle, which alleviates glutamate's neurotoxicity. To examine miR-9 targeting of GOT in the context of ischemic stroke, C57BL/6 mice were employed as an *in vivo* model. The mice were first cranially injected with either a GFP-tagged miR-9 inhibitor lentiviral vector or a non-

targeting scramble control vector. These vectors were delivered to the somatosensory (S1) cortex of the anticipated the stroke-affected hemisphere via stereotaxic injection. After 72 hours of delivery, ischemic stroke was induced in the mice via MCAO for 60 minutes. T2-weighted MRI was employed to determine the lesion volume of the stroke-affected hemisphere 48 hours later. After MRI, the brains were removed from the skulls, embedded in OCT, sectioned onto slides, and stained with an anti-GOT antibody.

Microscopic visualization of GFP (green) and GOT (red) in stroke-affected mouse brain confirmed successful delivery of lentiviral vectors. (**Figure 15A)**. Furthermore, fluorescence microscopy allowed us to quantify GOT expression in the two groups. GOT expression was significantly upregulated in the brains of mice receiving the miR-9 inhibitor lentiviral vector compared to those receiving the scramble control **(Figure 15B)**. These results support targeting of GOT by miR-9 *in vivo*.

Our lab has previously shown that induction of GOT expression during ischemic stroke attenuates lesion volume in the stroke-affected hemisphere[13]. In the current study, T2-weighted MRI showed that stroke-induced lesion volume was significantly reduced in mice receiving the miR-9 inhibitor lentiviral vector compared to controls. The images obtained from MRI are shown in **Figure 15C**, and quantification of the lesion volume is shown in **Figure 15D**. Taken together, the results from the *in vivo* model not only demonstrate that miR-9 targets GOT, but that GOT's neuroprotective properties in the context of ischemic stroke are enhanced when miR-9 expression is inhibited.

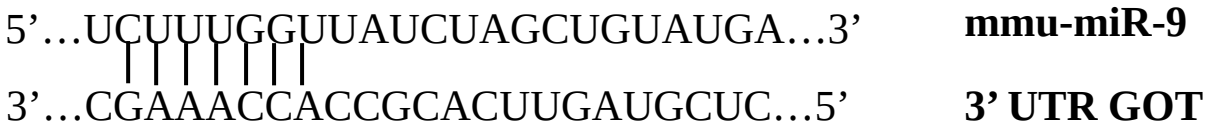

Figure 12: *In silico* sequence complementarity of GOT 3’ UTR and miR-9. Targetscan Mouse (ver 5.1) and miRanda were queried for complementarity of miR-9 binding to the 3’UTR of GOT (NM_010324). Both returned a single site of complementarity between bases 24-30 of the 3’UTR of GOT and based 2-8 of miR-9. This corresponds to the seed sequence of miR-9. Vertical lines represent perfect complementary binding.

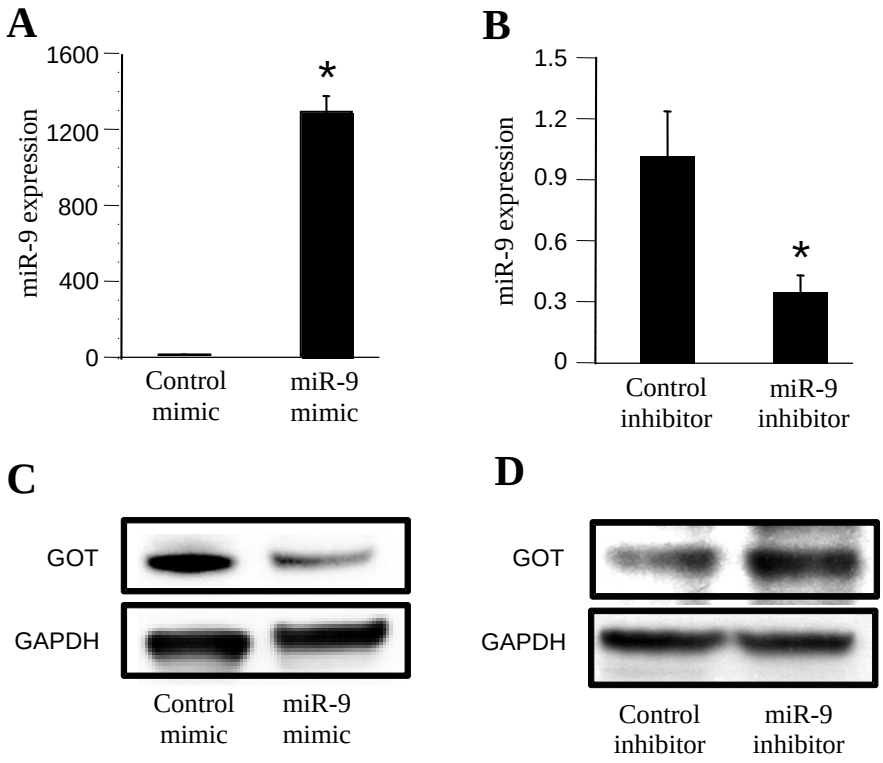

Figure 13: miR-9 targets GOT *in vitro*. Mouse hippocampal HT4 cells were transfected with either miRIDIAN mmu-miR-9 mimic, miRIDIAN miR-9 inhibitor, control mimic, or control inhibitor. miR-9 expression levels were measured in cells 72 hours post-transfection. miR-9 expression was significantly increased in miR-9 mimic cells compared to controls **(A)**, and significantly reduced in miR-9 inhibitor cells compared to controls **(B)**. Western blot was used to determine relative levels of GOT expression. Here, GAPDH was used as a housekeeping protein to confirm gel loading efficacy. GOT expression was reduced in miR-9 mimic cells compared to controls **(C)**, and increased in miR-9 inhibitor cells compared to controls **(D)**. *$p<0.05$.

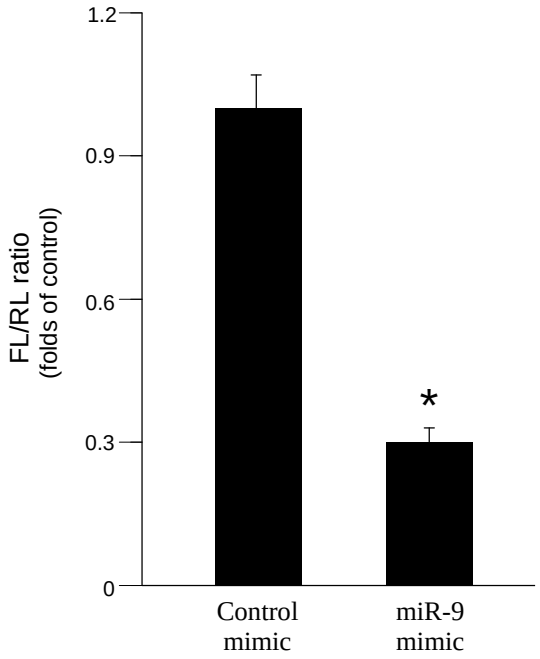

Figure 14: miR-9 targeting of GOT *in vitro.* After 72 hours of transfection, cells transfected with miRIDIAN mmu-miR-9 mimic or control mimic were co-transfected with pLuc-GOT—3'UTR plasmid and control plasmid for 24 hours. The GOT plasmid construct contained Firefly luciferase, while the control plasmid construct contained *Renilla* luciferase. After 24 hours, a dual luciferase assay was performed to measure GOT activity. The data are reported as Firefly:*Renilla* luciferase activity, with a greater ratio corresponding to greater GOT expression. The ratio of Firefly:*Renilla* luciferase activity was significantly reduced in miR-9 mimic cells compared to controls. *$p<0.01$.

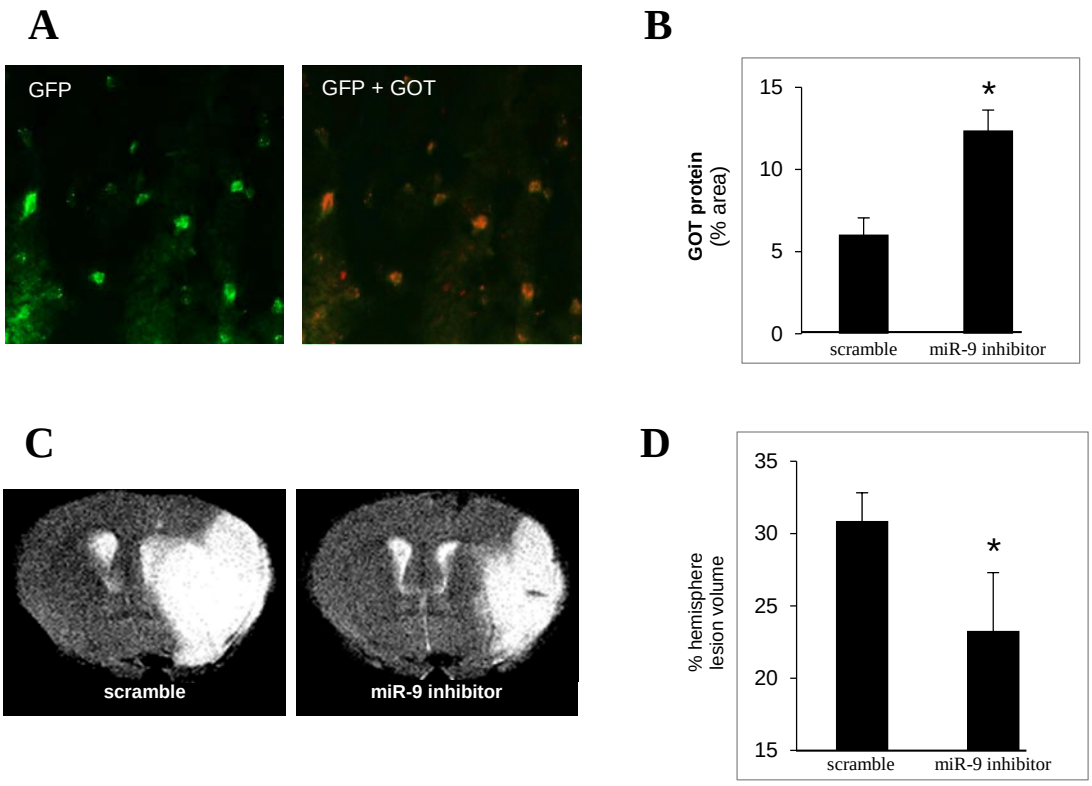

Figure 15: Inhibition of miR-9 upregulated GOT expression and reduced stroke-induced lesion volume. C57BL/6 mice were cranially injected with either GFP-tagged miR-9 inhibitor lentiviral particles or a non-targeting scramble control for 72 hours. Lentiviral vectors were delivered to the somatosensory cortex via stereotaxic injection. After 72 hours, ischemic stroke was induced via MCAO for 60 minutes. 48 hours after MCAO, T2-weighted MRI was performed, followed by removal and sectioning of the brain tissue for immunofluorescent analysis. Cells co-expressed GOT (red) and GFP (green), indicating successful uptake of lentiviral vectors **(A)**. GOT expression was significantly increased in mice receiving miR-9 inhibitor lentiviral vector compared to controls **(B)**. The lesion volume in the stroke hemisphere was significantly reduced mice receiving miR-9 inhibitor lentiviral vector compared to controls. **(C)** Representative images taken using T2-weighted MRI, **(D)** quantification of stroke-induced lesion volume. *$p<0.05$.

Discussion

As previously mentioned, stroke is the fifth leading cause of death in the United States[1]. The impact of this disease on American society and the healthcare system has motivated our lab to investigate mechanisms of improving post-stroke outcome. Given glutamate's well established role in the ischemic pathophysiological cascade, a myriad of studies have been carried out that have investigated ways to sequester neurotoxic glutamate from the synapse during stroke[5]. These include developing drugs that block the glutamatergic NMDA and AMPA receptors, block presynaptic calcium channels, or upregulate the EAATs that transport glutamate intracellularly from the synapse to glial cells. While these studies have shown promise in rodent models, they have so far failed to translate to clinical success[9,10,11].

A transcriptome screening previously performed by our lab demonstrated that correction of hypoxia during ischemic stroke induces expression of the glutamate-metabolizing enzyme GOT in the stroke-affected hemisphere of rats and mice[12]. GOT catalyzes the transfer of the amino group from glutamate to the 4-carbon TCA cycle intermediate oxaloacetate to form aspartate and the 5-carbon TCA cycle intermediate α-ketoglutarate. Subsequent work in our lab showed that SO therapy reduces glutamate levels and maintains normal ATP levels in the stroke-affected hemisphere of rats[13]. Furthermore, our lab demonstrated that lentiviral overexpression of GOT in the stroke-affected hemisphere of mice leads attenuates stroke-induced lesion volume, while knockdown of GOT exacerbates lesion volume[13]. These results support the idea that induction of GOT expression protects the brain from injury during ischemic stroke by metabolizing glutamate into the TCA cycle.

While studies dealing with glutamatergic receptors, calcium channels, and glial transporters have solely focused on removing excess glutamate from the synapse, our approach addresses two major factors that contribute to the pathophysiological cascade of ischemic stroke. By metabolizing glutamate into the TCA cycle, GOT simultaneously sequesters glutamate from the synapse and converts it into a metabolic fuel that can restore ATP production in neurons under ischemic conditions. This is essential because the lack of blood flow prevents glucose—the brain's primary metabolic fuel—from being delivered to the cells.

The purpose of the current study was to investigate other factors that may influence GOT expression. miRNAs are a class of small non-coding RNAs that play an important role in gene regulation. They do so by binding to the 3' UTR of the mRNAs of the genes that they target, leading to post-transcriptional gene silencing. miR-9 is abundantly expressed in brain tissue, and is predicted to target genes that play a role in glutamate metabolism. We therefore hypothesized that miR-9 targets GOT. The computational algorithms TargetScan Mouse and miRanda were used to search for regions of complementarity between the 3'UTR of GOT and miR-9. The seed sequence of miR-9 showed perfect complementarity with bases 24-30 of the 3' UTR of GOT. No other regions of complementarity were found. This type of binding between a miRNA and its mRNA target is characteristic of a 5'-dominant seed-only target site, and is sufficient to allow for mRNA targeting.

To biologically validate GOT as a target of miR-9, an *in vitro* and an *in vivo* model were employed. For the former, simulation of miR-9 overexpression in mouse hippocampal HT4 cells significantly decreased GOT expression. For the latter, inhibition of miR-9 in mice afflicted with

ischemic stroke significantly increased GOT expression and attenuated stroke-induced lesion volume. These results support targeting of GOT by miR-9, and that miR-9 inhibition enhances GOT's neuroprotective properties in the context of ischemic stroke.

Future studies in our lab will investigate the effect miR-9 inhibition on post-stroke outcome in mice. This could be performed by assessing sensorimotor function in mice before and after MCAO. Metrics such as distance travelled and average speed could be measured in a controlled environment over a predetermined amount of time pre- and post-stroke. Statistical analysis of the data collected could then determine if there is a significant post-stroke difference in these metrics in mice receiving miR-9 inhibitor lentiviral particles compared to controls. With promising results, drugs can be designed to inhibit miR-9 expression. There is already an ongoing effort to investigate natural products, such as curcumin, that may inhibit miRNAs believed to play a role in cancer progression[45]. This approach may perhaps be applied in the context of ischemic stroke as well. Our work with GOT so far has shown promising results in the effort to protect the brain from injury under ischemic conditions. This work presents a potential therapeutic opportunity in which a mechanism of GOT induction—such as miR-9 inhibition—could lead to an improved outcome for patients who suffer an ischemic stroke.

References

1. “Stroke Facts.” Centers for Disease Control and Prevention, 24 Mar. 2015. Web. 6 Apr. 2016. http://www.cdc.gov/stroke/facts.htm.
2. CDC, NCHS. Underlying Cause of Death 1999-2013 on CDC WONDER Online Database, released 2015. Data are from the Multiple Cause of Death Files, 1999-2013, as compiled from data provided by the 57 vital statistics jurisdictions through the Vital Statistics Cooperative Program. Accessed Feb. 3, 2015.
3. Mozaffarian D, Benjamin EJ, Go AS, et al. Heart disease and stroke statistics—2015 update: a report from the American Heart Association. *Circulation*. 2015; e29-322.
4. *Pubmed*. US National Library of Medicine, National Institutes of Health, 2016. Web. 6 Apr. 2016. http://www.ncbi.nlm.nih.gov/pubmed/?term=stroke.
5. Khanna S, Briggs Z, and Rink C. Inducible Glutamate Oxaloacetate Transaminase as a Therapeutic Target Against Ischemic Stroke. *Antioxid Redox Signal* 22: 175-186, 2015.
6. McEntee WJ and Crook TH. Glutamate: its role in learning, memory, and the aging brain. *Psychopharmacology* 111: 391-401, 1993.
7. Danbolt NC, Storm-Mathisen J, and Kanner BI. An [Na+ +K+]coupled L-glutamate transporter purified from rat brain is located in glial cell processes. *Neuroscience* 51: 295–310, 1992.
8. Tanaka K, Watase K, Manabe T, Yamada K, Watanabe M, Takahashi K, Iwama H, Nishikawa T, Ichihara N, Kikuchi T, Okuyama S, Kawashima N, Hori S, Takimoto M, and Wada K. Epilepsy and exacerbation of brain injury in mice lacking the glutamate transporter GLT-1. *Science* 276: 1699–1702, 1997.

9. Cheng YD, Al-Khoury L, and Zivin JA. Neuroprotection for ischemic stroke: two decades of success and failure. *NeuroRx* 1: 36–45, 2004.
10. Gladstone DJ, Black SE, and Hakim AM. Toward wisdom from failure: lessons from neuroprotective stroke trials and new therapeutic directions. *Stroke* 33: 2123–2136, 2002.
11. Radermacher KA, Wingler K, Kleikers P, Altenhofer S, Hermans J, Jr, Kleinschnitz C, and Hhw Schmidt H. The 1027th target candidate in stroke: will NADPH oxidase hold up? *Exp Transl Stroke* Med 4: 11, 2012.
12. Rink C, Roy S, Khan M, Ananth P, Kuppusamy P, Sen CK, and Khanna S. Oxygen-sensitive outcomes and gene expression in acute ischemic stroke. *J Cereb Blood Flow Metab* 30: 1275-1287, 2010.
13. Rink C, Gnyawali S, Peterson L, and Khanna S. Oxygen-Inducible Glutamate Oxaloacetate Transaminase as Protective Switch Transforming Neurotoxic Glutamate to Metabolic Fuel During Acute Ischemic Stroke. *Antioxid Redox Signal* 14: 1777-1785, 2011.
14. Bartel DP. MicroRNAs: Genomics, Biogenesis, Mechanism, and Function. *Cell* 116: 281-297, 2004.
15. Yi R, Qin Y, Macara IG, and Cullen BR. Exportin-5 mediates the nuclear export of pre-microRNAs and short hairpin RNAs. *Genes Dev* 17:3011–3016, 2003.
16. Lund E, Güttinger S, Calado A, Dahlberg JE, and Kutay U. Nuclear export of microRNA precursors. *Science* 303: 95–98, 2004.
17. Lau NC, Lim LP, Weinstein EG, and Bartel DP. An abundant class of tiny RNAs with probable regulatory roles in *Caenorhabditis elegans*. *Science* 294: 858–862, 2001.

18. Dalmay T. Mechanism of miRNA-mediated repression of mRNA translation. *Essays Biochem* 54: 29-38, 2013.
19. Coolen M, Katz S, and Bally-Cuif. miR-9: a versatile regulator of neurogenesis. *Front Cell Neurosci* 7: 1-11, 2013.
20. Buckley NJ, Johnson R, Zuccato C, Bithell A, and Cattaneo E. The role of REST in transcriptional and epigenetic dysregulation in Huntington's disease. *Neurobiol Dis* 39: 28-39, 2010.
21. Packer AN, Xing Y, Harper SQ, Jones L, and Davidson BL. The bifunctional microRNA miR-9/miR-9* regulates REST and CoREST and is downregulated in Huntington's disease. *J Neurosci* 28: 14341-14346, 2008.
22. Laneve P, Gioia U, Andriotto A, Moretti F, Bozzoni I, and Caffarelli E. A minicircuitry involving REST and CREB controls miR-9-2 expression during human neuronal differentiation. *Nucleic Acids Res* 38: 6895-6905, 2010.
23. Cogswell JP, Ward J, Taylor IA, Water M, Shi Y, Cannon B, Kelnar K, Kemppainen J, Brown D, Chen C, Prinjha RK, Richardson JC, Saunders AM, Roses AD, and Richards CA. Identification of miRNA changes in Alzheimer's disease brain and CSF yields putative biomarkers and insights into disease pathways. *J Alzheimers Dis* 14: 27-41, 2008.
24. Hébert SS, Horré K, Nicolaï L, Papadopoulou AS, Mandemakers W, Silahtaroglu AN, Kauppinen S, Delacourte A, and De Strooper B. Loss of microRNA cluster miR-29a/b-1 in sporadic Alzheimer's disease correlates with increased BACE1/beta-secretase expression. *Proc Natl Acad Sci USA* 105: 6415-6420, 2008.

25. Haramati S, Chapnik E, Sztainberg Y, Eilam R, Zwang R, Gershoni N, McGlinn E, Heiser PW, Wills AM, Wirguin I, Rubin LL, Misawa H, Tabin CJ, Brown R Jr, Chen A, and Hornstein E. miRNA malfunction causes spinal motor neuron disease. *Proc Natl Acad Sci USA* 107: 13111-13116, 2010.
26. Kim J, Inoue K, Ishii J, Vanti WB, Voronov SV, Murchison E, Hannon G, and Abeliovich A. A MicroRNA feedback circuit in midbrain dopamine neurons. *Science* 317: 1220-1224, 2007.
27. Rink C and Khanna S. MicroRNA in ischemic stroke etiology and pathology. *Physiol Genomics* 43: 521-528, 2011.
28. Wei N, Xiao L, Xue R, Zhang D, Zhou J, Ren H, Guo S, and Xu J. MicroRNA-9 Mediates the Cell Apoptosis by Targeting Bcl2l11 in Ischemic Stroke. *Mol Neurobiol*. 2015.
29. Ji R, Cheng Y, Yue J, Yang J, Liu X, Chen H, Dean DB, and Zhang C. MicroRNA expression signature and antisense-mediated depletion reveal an essential role of MicroRNA in vascular neointimal lesion formation. *Circ Res* 100: 1579-1588, 2007.
30. Weber M, Baker MB, Moore JP, and Searles CD. MiR-21 is induced in endothelial cells by shear stress and modulates apoptosis and eNOS activity. *Biochem Biophys Res Commun* 393: 643-648, 2010.
31. Harris TA, Yamakuchi M, Ferlito M, Mendell JT, and Lowenstein CJ. MicroRNA-126 regulates endothelial expression of vascular cell adhesion molecule 1. *Proc Natl Acad Sci USA* 105: 1516-1521, 2008.

32. Wang S, Aurora AB, Johnson BA, Qi X, McAnally J, Hill JA, Richardson JA, Bassel-Duby R, and Olson EN. The endothelial-specific microRNA miR-126 governs vascular integrity and angiogenesis. *Dev Cell* 15: 261-271, 2008.
33. Rayner KJ, Suarez Y, Davalos A, Parathath S, Fitzgerald ML, Tamehiro N, Fisher EA, Moore KJ, and Fernandez-Hernando C. MiR-33 contributes to the regulation of cholesterol homeostasis. *Science* 328: 1570-1573, 2010.
34. Chen T, Huang Z, Wang L, Wang Y, Wu F, Meng S, and Wang C. MicroRNA-125a-5p partly regulates the inflammatory response, lipid uptake, and ORP9 expression in oxLDL-stimulated monocyte/macrophages. *Cardiovasc Res* 83: 131-139, 2009.
35. Martin MM, Buckenberger JA, Jiang J, Malana GE, Nuovo GJ, Chotani M, Feldman DS, Schmittgen TD, and Elton TS. The human angiotensin II type 1 receptor +1166 A/C polymorphism attenuates microRNA-155 binding. *J Biol Chem* 282: 24262-24269, 2007.
36. Xu CC, Han WQ, Xiao B, Li NN, Zhu DL, and Gao PJ. [Differential expression of microRNAs in the aorta of spontaneously hypertensive rats.]. *Sheng Li Xue Bao* 60: 553-560, 2008.
37. Dentelli P, Rosso A, Orso F, Olgasi C, Taverna D, and Brizzi MF. microRNA-222 controls neovascularization by regulating signal transducer and activator of transcription 5A expression. *Arterioscler Thromb Vasc Biol* 30: 1562-1568, 2010.
38. Poliseno L, Tuccoli A, Mariani L, Evangelista M, Citti L, Woods K, Mercatanti A, Hammond S, and Rainaldi G. MicroRNAs modulate the angiogenic properties of HUVECs. *Blood* 108: 3068-3071, 2006.
39. Fasanaro P, D'Alessandra Y, DiStefano V, Melchionna R, Romani S, Pompilio G, Capogrossi MC, and Martelli F. MicroRNA-210 modulates endothelial cell response to

hypoxia and inhibits the receptor tyrosine kinase ligand Ephrin-A3. *J Biol Chem* 283: 15878-15883, 2008.

40. Fasanaro P, Greco S, Lorenzi M, Pescatori M, Brioschi M, Kulshreshtha R, Banfi C, Stubbs A, Calin GA, Ivan M, Capogrossi MC, and Martelli F. An integrated approach for experimental target identification of hypoxia-induced miR-210. *J Biol Chem* 284: 35134-35143, 2009.
41. Yin KJ, Deng Z, Hamblin M, Xiang Y, Huang H, Zhang J, Jiang X, Wang Y, and Chen YE. Peroxisome proliferator-activated receptor delta regulation of miR-15a in ischemia-induced cerebral vascular endothelial injury. *J Neurosci* 30: 6398-6408, 2010.
42. Yin KJ, Deng Z, Huang H, Hamblin M, Xie C, Zhang J, Chen YE. miR-497 regulates neuronal death in mouse brain after transient focal cerebral ischemia. *Neurobiol Dis* 38: 17-26, 2010.
43. Khanna S, Rink C, Ghoorkhanian R, Gnyawali S, Heigel M, Wijesinghe DS, Chalfant CE, Chan YC, Banerjee J, Huang Y, Roy S, and Sen CK. Loss of miR-29b following acute ischemic stroke contributes to neural cell death and infarct size. *J Cereb Blood Flow Metab* 33: 1197-1206, 2013.
44. Chan YC, Khanna S, Roy S, and Sen CK. miR-200b targets Ets-1 and is down-regulated by hypoxia to induce angiogenic response of endothelial cells. *J Biol Chem* 286: 2047-2056, 2011.
45. Li Y, Kong D, Wang Z, and Sarka FH. Regulation of microRNAs by Natural Agents: An Emerging Field in Chemoprevention and Chemotherapy Research. *Pharm Res* 27: 1027-1041, 2010.